

Molecular Meccano, 49<sup>[†]</sup>

## Pseudorotaxanes and Catenanes Containing a Redox-Active Unit Derived from Tetrathiafulvalene

Masumi Asakawa,<sup>[a]</sup> Peter R. Ashton,<sup>[a]</sup> Vincenzo Balzani,<sup>\*,[b]</sup> Sue E. Boyd,<sup>[a]</sup>  
 Alberto Credi,<sup>[b]</sup> Gunter Matternsteig,<sup>[a],[†]</sup> Stephan Menzer,<sup>[c]</sup> Marco Montalti,<sup>[b]</sup>  
 Francisco M. Raymo,<sup>[a],[†]</sup> Cristina Ruffilli,<sup>[b]</sup> J. Fraser Stoddart,<sup>\*,[a],[†]</sup>  
 Margherita Venturi,<sup>[b]</sup> and David J. Williams<sup>\*,[c]</sup>

**Keywords:** Catenanes / Molecular machines / Pseudorotaxanes / Template-directed synthesis / Tetrathiafulvalenes

Two bis(2-oxy-1,3-propylenedithio)tetrathiafulvalene-containing acyclic polyethers and two macrocyclic polyethers, each incorporating one bis(2-oxy-1,3-propylenedithio)tetrathiafulvalene unit and one *p*-phenylene ring, have been synthesized. The two acyclic polyethers are bound by cyclobis(paraquat-*p*-phenylene) with pseudorotaxane geometries in solution. The two macrocyclic polyethers have been mechanically interlocked with this tetracationic cyclophane to form [2]catenanes in a kinetically controlled self-assembly process. The X-ray crystallographic analysis of one of the two [2]catenanes and <sup>1</sup>H-NMR-spectroscopic studies of both compounds showed that the *p*-phenylene ring of the macrocyclic polyether is located inside the cavity of the tetracationic cyclophane, while the bis(2-oxy-1,3-propylenedithio)tetrathiafulvalene unit resides alongside. The [2]pseudorotaxanes and [2]catenanes show broad bands around 780 nm, arising from the charge-transfer (CT) interaction between the electron-donor tetrathiafulvalene-(TTF)-type unit and the electron-acceptor units of the tetracationic cyclophane. <sup>1</sup>H-NMR-spectroscopic studies have shown that the [2]pseudorotaxanes dissociate into their

separate components upon oxidation of the TTF-type unit, as a result of disruption of the CT interaction and electrostatic repulsion between the tetracationic host and the newly formed monocationic guest. The subsequent reduction of the guest to its neutral state affords back the pseudorotaxane-type complex restoring the original equilibrium. The results obtained from electrochemical experiments are consistent with the reversible, redox-driven dethreading/rethreading process observed by <sup>1</sup>H-NMR spectroscopy. Variable-temperature <sup>1</sup>H-NMR-spectroscopic investigations have revealed two dynamic processes, both involving the relative movements of the mechanically interlocked components in the [2]catenanes. The two consecutive oxidation processes involving the TTF-type unit, observed electrochemically, are displaced toward more positive potentials compared with the free cyclic polyethers. The two reversible two-electron reduction processes, characteristic of free cyclobis(paraquat-*p*-phenylene), separate into four reversible one-electron processes because of the topological difference between the "inside" and "alongside" electron-acceptor units in the [2]catenane.

## Introduction

The reversible oxidation of tetrathiafulvalene (TTF) to its radical monocation can be realized<sup>[1]</sup> both chemically and electrochemically. As a result, TTF is an ideal building block<sup>[2]</sup> for the construction of redox-active molecular and supramolecular systems<sup>[3]</sup> which can be controlled by exter-

nal stimuli. The observation that TTF – in its neutral state – is bound<sup>[4]</sup> by the tetracationic cyclophane, cyclobis(paraquat-*p*-phenylene), with a pseudorotaxane geometry prompted<sup>[5]</sup> us and others to design and construct TTF-containing mechanically interlocked molecules<sup>[6]</sup> and their supramolecular analogs. The tetracationic nature of cyclobis(paraquat-*p*-phenylene), in conjunction with the possibility of converting the neutral TTF unit to its monocation and back again, offers the opportunity for controlling the relative positions of the components in catenanes, rotaxanes, and pseudorotaxanes.<sup>[7]</sup> Thus, we have designed and constructed two TTF-containing [2]catenanes and two related [2]pseudorotaxanes. Here, we report (i) the syntheses of two acyclic and two macrocyclic bis(2-oxy-1,3-propylenedithio)TTF-containing polyethers, (ii) the template-directed syntheses of two [2]catenanes, each incorporating one of these macrocycles and cyclobis(paraquat-*p*-phenylene), (iii) the X-ray-crystallographic analysis of one of the [2]catenanes, (iv) the <sup>1</sup>H-NMR-spectroscopic investigations of both [2]catenanes, (v) the absorption spectra, and the elec-

[†] Part 48: P. R. Ashton, J. A. Bravo, F. M. Raymo, J. F. Stoddart, A. J. P. White, D. J. Williams, *Eur. J. Org. Chem.* **1999**, 899–908.

[†] Current address: Department of Chemistry and Biochemistry, University of California, Los Angeles, 405 Hilgard Avenue, Los Angeles, California 90095-1569, USA Fax: (internat.) + 1-310/206-1843 E-mail: stoddart@chem.ucla.edu

[a] School of Chemistry, University of Birmingham, Edgbaston, Birmingham B15 2TT, UK

[b] Dipartimento di Chimica "G. Ciamician", Università di Bologna, Via Selmi 2, I-40126 Bologna, Italy Fax: (internat.) + 39-051/259456

[c] Department of Chemistry, Imperial College, South Kensington, London SW7 2AY, UK Fax: (internat.) + 44-171/594-5835

trochemical oxidation and reduction behavior of the acyclic and macrocyclic bis(2-oxy-1,3-propylenedithio)TTF-containing polyethers, and of their pseudorotaxanes and of two [2]catenanes, respectively, incorporating cyclobis(paraquat-*p*-phenylene), and (vi) the oxidation/reduction controllable decomplexation/recomplexation of the acyclic TTF-containing polyethers by cyclobis(paraquat-*p*-phenylene).

## Results and Discussion

### Synthesis

A mixture of the *cis* and the *trans* isomers<sup>[8]</sup> of **1** was treated (Scheme 1) with either **2** or **3** to afford **4** or **5**, respectively. After deprotection of **4** and **5**, the resulting compounds **6** and **7** were allowed to react with 1,4-bis(bromomethyl)benzene under high-dilution conditions to give the macrocyclic polyethers **8** and **9**, respectively. Reaction of  $10 \cdot 2 \text{ PF}_6^-$  with 1,4-bis(bromomethyl)benzene, in the presence of either **8** or **9**, afforded the [2]catenanes **11**  $\cdot 4 \text{ PF}_6^-$  or **12**  $\cdot 4 \text{ PF}_6^-$ , respectively, after counterion exchange.

### X-ray Crystallography

The X-ray crystallographic analysis of the [2]catenane **11**  $\cdot 4 \text{ PF}_6^-$  shows (Figure 1) the *p*-phenylene ring of the macrocyclic polyether to be threaded through the center of the tetracationic cyclophane. The  $\text{CH}_2\text{--C}_6\text{H}_4\text{--CH}_2$  axis is inclined steeply ( $70^\circ$ ) to the mean plane of the tetracationic

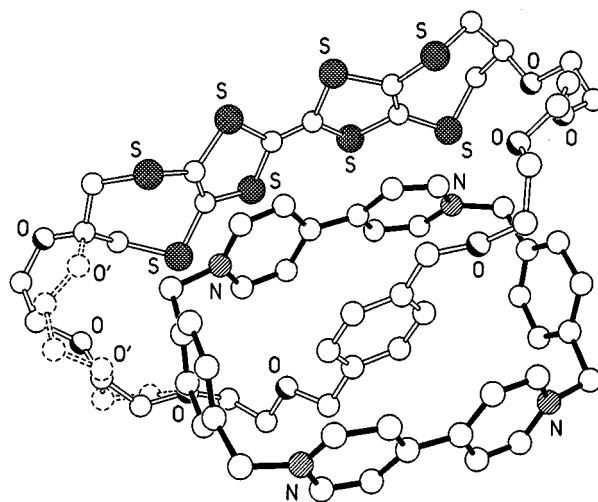
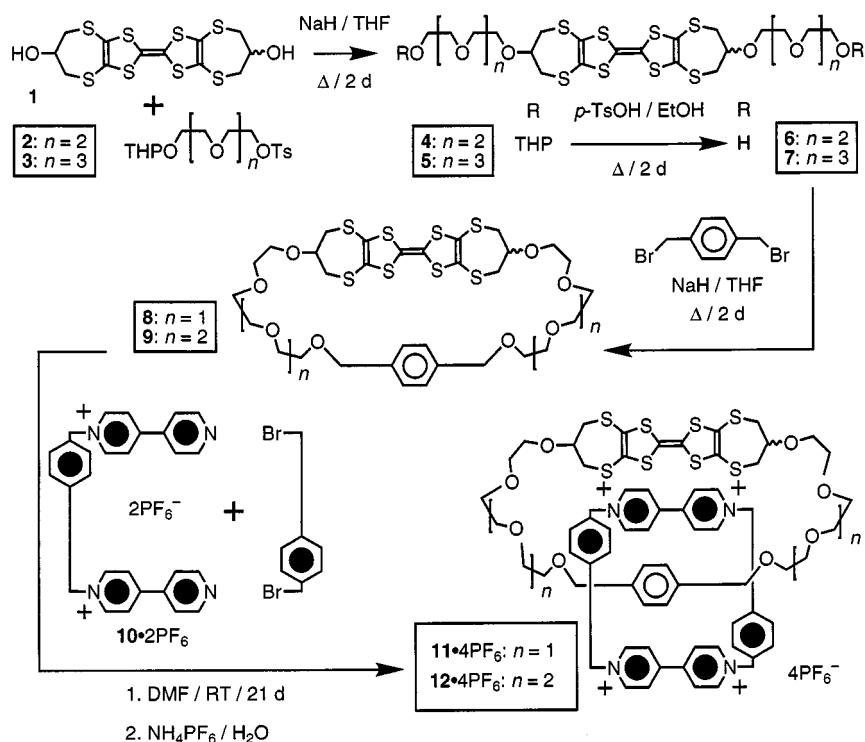


Figure 1. Ball-and-stick representation of the solid-state structure of the [2]catenane **11**<sup>4+</sup>.

cyclophane (defined by the four methylene carbon atoms), while the long axis of the TTF unit is aligned almost parallel ( $18^\circ$ ) to the N–N axis of the proximal bipyridinium unit. An important feature of the macrocyclic polyether is the presence of 50:50 disorder in one of the polyether chains (depicted by broken bonds in Figure 1). This disorder reflects the presence of *cis/trans* isomerism as a consequence of a formal configurational inversion at one of the bridgehead carbon atoms within the bis(2-oxy-1,3-propylenedithio)TTF unit. The [2]catenane is stabilized by  $\pi\cdots\pi$  stacking interactions, between the *p*-phenylene ring and the two bipyridinium units, and, by edge-to-face interactions, be-



Scheme 1. The syntheses of the compounds **4**–**12**  $\cdot 4 \text{ PF}_6^-$ .

tween the *p*-xylene ring of the macrocyclic polyether and the *p*-phenylene rings of the tetracationic cyclophane.<sup>[9]</sup> There is evidence for two short C–H···O contacts, one between one of the  $\alpha$ -bipyridinium hydrogen atoms and one of the polyether oxygen atoms and the other between one of the proximal methylene hydrogen atoms and another oxygen atom in the same polyether chain.<sup>[10]</sup> The near parallel alignments of the long axes of the TTF unit and of the “inside” bipyridinium ring system could be a result of S(sp<sup>3</sup>)–N(p) interactions.<sup>[11]</sup> These sulfur atoms are in a pseudotrigonal-bipyramidal relationship with respect to the bipyridinium nitrogen atoms and their substituents. The S–N distances are 3.54 and 3.37 Å, respectively. There are no extended  $\pi$ -donor/ $\pi$ -acceptor stacks formed within the crystal of **11** · 4 PF<sub>6</sub>. The molecules pack (Figure 2) to form discrete face-to-face “dimer pairs” with the TTF units aligned parallel but offset longitudinally. Their C=C bonds have a perpendicular separation<sup>[12]</sup> of 3.52 Å and an associated centroid–centroid distance of 3.71 Å. There are no bipyridinium–bipyridinium stacking interactions of the

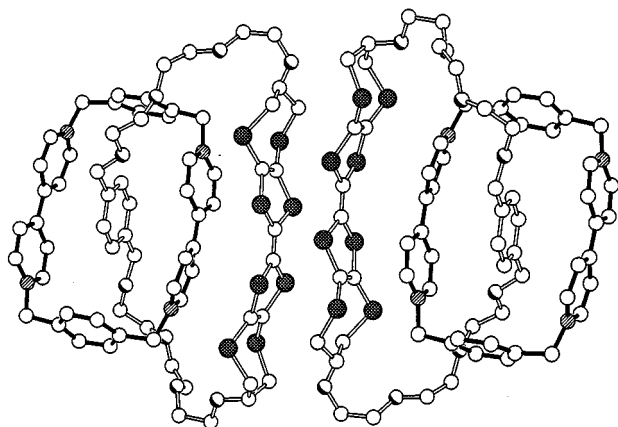


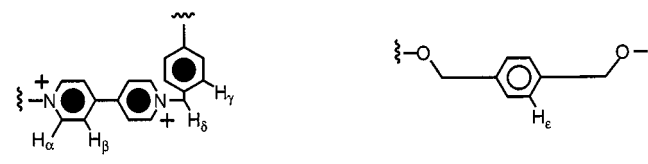
Figure 2. One of the “dimer pairs” formed by the [2]catenane **11**<sup>4+</sup> in the crystal

type seen, for example, in the solid-state structure of cyclo-bis(paraquat-1,4-biphenylene).<sup>[13]</sup>

### <sup>1</sup>H-NMR Spectroscopy

Comparison of the <sup>1</sup>H-NMR spectra [(CD<sub>3</sub>)<sub>2</sub>CO, 298 K] of the macrocyclic polyethers **8** and **9** with those of the corresponding [2]catenanes **11** · 4 PF<sub>6</sub> and **12** · 4 PF<sub>6</sub> revealed (Table 1) dramatic shifts of the resonances associated with the aromatic protons of the *p*-phenylene ring incorporated within the neutral macrocyclic components. By contrast, no significant chemical shift changes were observed for the signals associated with the protons of the bis(2-oxy-1,3-propylenedithio)TTF unit.<sup>[14]</sup> These observations suggest that in solution the tetracationic cyclophane also encircles preferentially the *p*-phenylene ring in both [2]catenanes.

Table 1. <sup>1</sup>H-NMR-spectroscopic data ( $\delta$  values) for **8**, **9**, and **11** · 4 PF<sub>6</sub> to **13** · 4 PF<sub>6</sub> in (CH<sub>3</sub>)<sub>2</sub>CO at 298 K

Compound					
	H <sub><math>\alpha</math></sub>	H <sub><math>\beta</math></sub>	H <sub><math>\gamma</math></sub>	H <sub><math>\delta</math></sub>	H <sub><math>\epsilon</math></sub>
<b>8</b>	—	—	—	—	7.30
<b>9</b>	—	—	—	—	7.30
<b>11</b> · 4 PF <sub>6</sub>	9.39	8.33	8.19	6.23	4.17
<b>12</b> · 4 PF <sub>6</sub>	9.38	8.32	8.16	6.19	4.17
<b>13</b> · 4 PF <sub>6</sub>	9.38	8.58	7.76	6.15	—

In both [2]catenanes, two dynamic processes (Figure 3) can be identified by variable-temperature <sup>1</sup>H-NMR spectroscopy. Process I involves the circumrotation of the tetracationic cyclophane through the cavity of the macrocyclic polyether. Process II involves the rocking of the

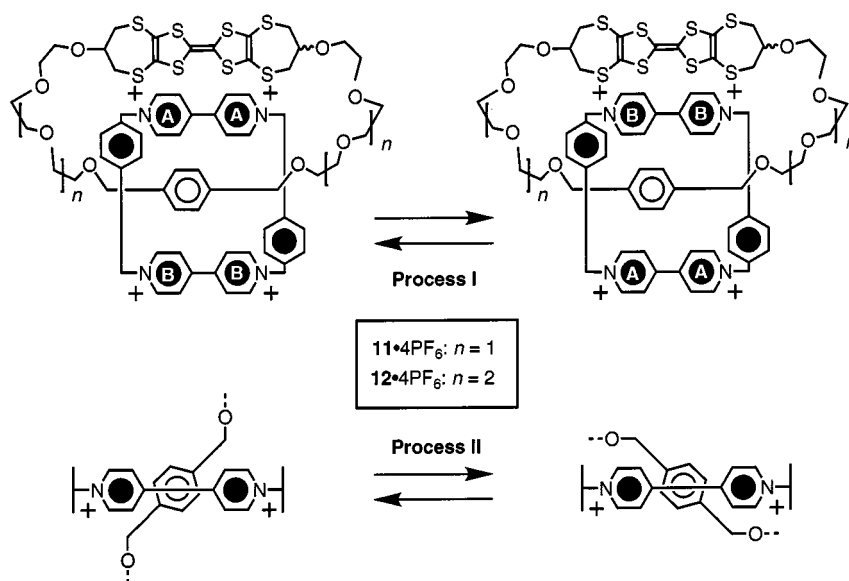


Figure 3. The dynamic processes associated with the [2]catenanes **11** · 4 PF<sub>6</sub> and **12** · 4 PF<sub>6</sub> in solution

$\text{CH}_2\text{--C}_6\text{H}_4\text{--CH}_2$  axis of the encircled *p*-phenylene ring relative to the mean plane of the tetracationic cyclophane as defined by the four methylene carbon atoms. At 193 K, Processes I and II are slow on the  $^1\text{H}$ -NMR timescale and four sets of resonances can be distinguished<sup>[15]</sup> (Figure 4e) for the  $\alpha$ -bipyridinium protons. In addition, two sets of signals centered on  $\delta \approx 5.3$  and 2.9 for the aromatic protons of the encircled *p*-phenylene ring pointing away and toward, respectively, the  $\pi$ -faces of the *p*-phenylene spacers of the tetracationic cyclophane are observed. Upon warming the solution up, Process II becomes faster and the two sets of signals associated with the encircled *p*-phenylene ring protons coalesce to give only one signal. Similarly, the two pairs of resonances for the  $\alpha$ -bipyridinium protons also coalesce (Figures 4c and 4d) to give one pair only. Upon further warming the solution up, Process I becomes faster and only one set of signals can be observed (Figures 4a and 4b) for the  $\alpha$ -bipyridinium protons.<sup>[16]</sup>

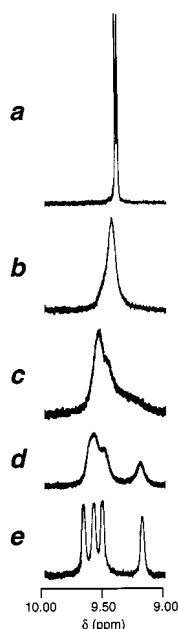


Figure 4. Partial  $^1\text{H}$ -NMR spectra of the [2]catenane **11**·4PF<sub>6</sub> in (CD<sub>3</sub>)<sub>2</sub>CO at (a) 293, (b) 233, (c) 215, (d) 203, and (e) 193 K, illustrating the resonances associated with the  $\alpha$ -bipyridinium protons

Upon mixing (Figure 5) equimolar amounts of the tetracationic cyclophane of **13**·4 PF<sub>6</sub> and either **6** or **7** in solution, a green color develops, indicating the formation of a complex having, presumably, a [2]pseudorotaxane geometry.<sup>[17]</sup> The  $^1\text{H}$ -NMR spectra of equimolar CD<sub>3</sub>CN/D<sub>2</sub>O (95:5) solutions of **13**·4 PF<sub>6</sub> and either **6** or **7** exhibit (Figure 6a) the signals of the complexed and uncomplexed species. In addition, since mixtures of the *cis* and the *trans* isomers of the guest were employed in the case of **6** and **7**, two distinct sets of resonances for the bipyridinium protons of the complexed tetracationic cyclophane can be distinguished. Upon addition of three molar equivalents of I<sub>2</sub>, the TTF unit is oxidized to the radical monocation and dissociation of the complex occurs as a result of the disruption of the CT interaction and the presence of electrostatic repulsion between the tetracationic host and the monoc-

ationic guest. In keeping with this observation, no complexed species can be detected (Figure 6b) in the  $^1\text{H}$ -NMR spectra. Upon addition of an excess of Na<sub>2</sub>S<sub>2</sub>O<sub>5</sub>/NH<sub>4</sub>PF<sub>6</sub>,

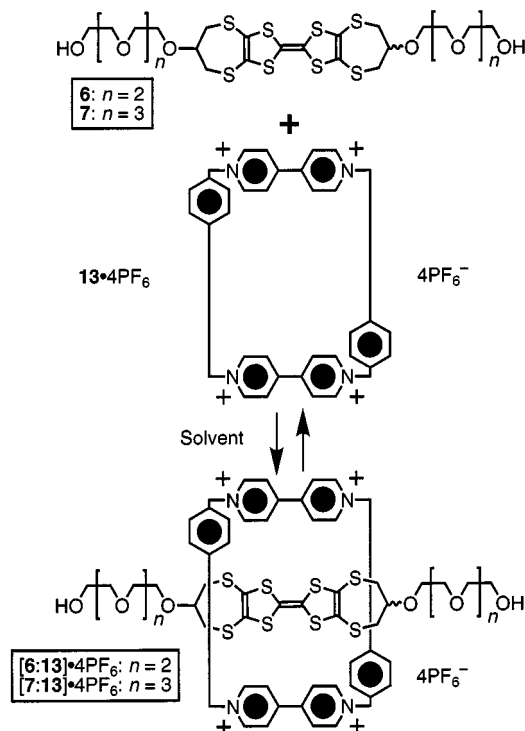


Figure 5. Complexation of **6** and **7** by the tetracationic cyclophane **13**·4 PF<sub>6</sub>

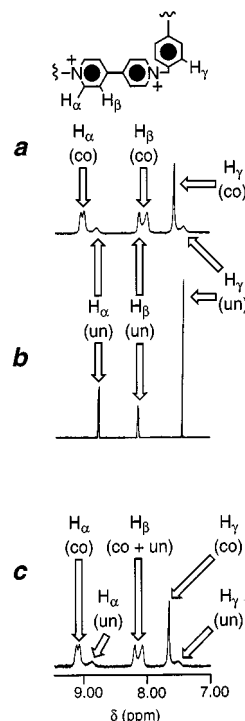


Figure 6. Partial  $^1\text{H}$ -NMR spectra of (a) an equimolar CD<sub>3</sub>CN/D<sub>2</sub>O (95:5) solution of **6** and **13**·4 PF<sub>6</sub>, (b) the same solution after the addition of I<sub>2</sub> (3 mol-equiv.) and then (c) of Na<sub>2</sub>S<sub>2</sub>O<sub>5</sub> (8 mol-equiv.) and NH<sub>4</sub>PF<sub>6</sub> (22 mol-equiv.); note that co ≡ complexed and un ≡ uncomplexed

the radical monocation is reduced back to its neutral state, thus resulting in the original equilibrium between complexed and uncomplexed species being restored as illustrated by the partial  $^1\text{H-NMR}$  spectrum depicted in Figure 6c for  $[\mathbf{6}:\mathbf{13}] \cdot 4 \text{PF}_6$ . More details on the redox-driven dissociation/reassociation process of the  $[\mathbf{6}:\mathbf{13}]^{4+}$  adduct will be given when discussing the electrochemical behavior of this [2]pseudorotaxane later on this paper.

### Absorption Spectra

As previously reported,<sup>[7k]</sup> the absorption spectrum of cyclobis(paraquat-*p*-phenylene) shows very intense bands in the UV region and no absorption in the visible region. The absorption band of the bis(2-oxy-1,3-propylenedithio)TTF-containing acyclic polyether **6** is shown in Figure 7, where the spectrum of the pseudorotaxane  $[\mathbf{6}:\mathbf{13}]^{4+}$  is also displayed. The broad band in the visible/near-IR spectral region of the pseudorotaxane ( $\lambda_{\text{max}} = 780 \text{ nm}$ ,  $\epsilon_{\text{max}} = 1300 \text{ M}^{-1} \text{ cm}^{-1}$ ) results from the charge-transfer interaction between the electron-donor TTF-type unit of **6** and the electron-acceptor units of  $\mathbf{13}^{4+}$ . The stability constant of  $[\mathbf{6}:\mathbf{13}]^{4+}$ , as measured from spectrophotometric titrations, is ca.  $1 \cdot 10^4 \text{ M}^{-1}$ .

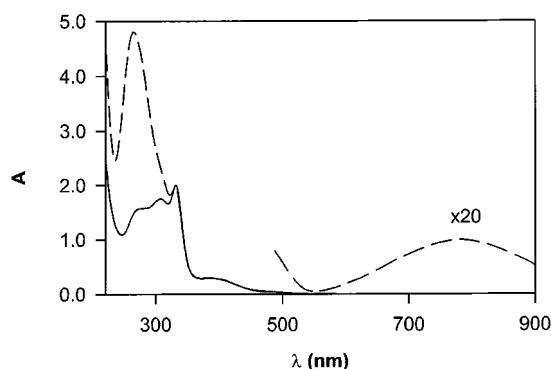


Figure 7. Absorption spectra of  $1.0 \cdot 10^{-4} \text{ M}$  MeCN solutions of **6** (full line) and a 1:1 mixture of **6** and  $\mathbf{13}^{4+}$  (dashed line); under these conditions, about 45% of the species are associated to give the pseudorotaxane  $[\mathbf{6}:\mathbf{13}]^{4+}$ .

The spectrum of the macrocyclic bis(2-oxy-1,3-propylenedithio)TTF-containing polyether **8** (Figure 8) differs from that of the acyclic polyether **6** (Figure 7) only in the region below 300 nm, where the phenylene unit present in **8** contributes to the absorption. This behavior shows that, as expected, there is no apparent electronic interaction between the TTF- and phenylene-type units in **8**. The spectrum of catenane  $\mathbf{11}^{4+}$  (Figure 8) shows a CT band ( $\lambda_{\text{max}} = 768 \text{ nm}$ ,  $\epsilon_{\text{max}} = 500 \text{ M}^{-1} \text{ cm}^{-1}$ ) similar to, but not identical to, that of pseudorotaxane  $[\mathbf{6}:\mathbf{13}]^{4+}$ . The observed differences, and particularly the much smaller  $\epsilon$  value, suggest that, in the catenane structure, contrary to what happens in the pseudorotaxane  $[\mathbf{6}:\mathbf{13}]^{4+}$ , the electron-acceptor cyclophane  $\mathbf{13}^{4+}$  does not surround the TTF-type unit of the macrocyclic polyether **8**. This conclusion is in full agreement with the results obtained by X-ray crystallography

and  $^1\text{H-NMR}$  spectra (vide supra), and also by electrochemistry (vide infra).

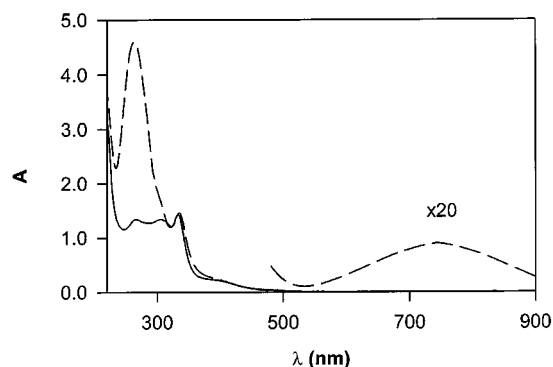


Figure 8. Absorption spectra in MeCN of **8** (full line) and the [2]catenane  $\mathbf{11}^{4+}$  (dashed line)

Oxidation of polyether **6** with  $\text{Fe}(\text{ClO}_4)_3$  in MeCN solution causes strong spectral changes (Figure 9). Up to 1 equiv. of oxidant, the disappearance of the TTF-type band in the near-UV spectral region is accompanied by the appearance of intense bands in the visible region, characteristic of monooxidized  $\text{TTF}^+$ -type species.<sup>[5b,18]</sup> Therefore, **6** is oxidized to  $\mathbf{6}^+$ , with maintenance of an isosbestic point at 353 nm (Figure 9a). Further addition of oxidant causes the disappearance of the bands of the monooxidized  $\text{TTF}^+$ -type species and the appearance of a new band around 580 nm, with isosbestic points at 355, 496, and 664 nm (Figure 9b). Such spectral changes can be assigned to the formation of  $\mathbf{6}^{2+}$ . Upon addition of a reductant (aqueous ascorbic acid) to the oxidized solution, the spectral changes are fully reversed. Interestingly, while the spectrum of  $\mathbf{6}^+$  is somewhat similar to that of  $\text{TTF}^+$ ,<sup>[5b,18]</sup> the spectrum of  $\mathbf{6}^{2+}$  differs from that of  $\text{TTF}^{2+}$ <sup>[5b,18]</sup> because of the presence

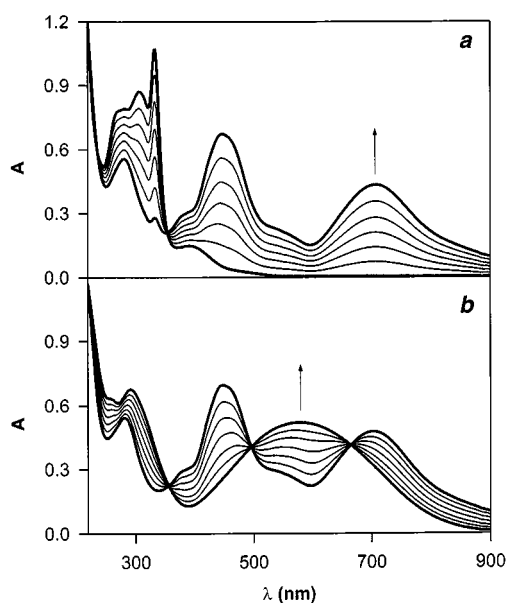


Figure 9. Spectral changes observed upon one-electron (a) and two-electron (b) oxidation of **6** [ $5 \cdot 10^{-5} \text{ M}$ , MeCN solution,  $\text{Fe}(\text{ClO}_4)_3$  as an oxidant]; the changes can be reversed by addition of a reductant (aqueous ascorbic acid)



of a broad band which extends from the visible to the near-IR. This behavior can be accounted for by the presence of the four alkylthio substituents attached to the TTF<sup>2+</sup>-type aromatic moiety in **6**<sup>2+</sup>. The sulfur atoms associated with these substituents carry nonbonding electron pairs and can therefore give rise to  $n\pi^*$  transitions (and absorption bands) at relatively low energy. The presence of such low-energy levels in **6**<sup>2+</sup> precludes, of course, the occurrence of emission from the upper-lying  $\pi\pi^*$  level, which is observed for TTF<sup>2+</sup>.<sup>[19]</sup>

The spectroscopic characteristics of the acyclic polyether **7**, the pseudorotaxane **[7:13]**<sup>4+</sup>, the macrocyclic polyether **9**, and the catenane **12**<sup>4+</sup> are practically identical to those of the corresponding compounds discussed in this section.

### Electrochemical Behavior

Both acyclic polyethers **6** and **7** show two reversible and monoelectronic oxidation processes at +0.54 V and +0.85 V (vs. SCE), which can be easily assigned to first and second oxidation of their TTF-type units, and no reduction processes. As a consequence of the identical electrochemical behavior of these two parent species, the corresponding pseudorotaxanes, macrocycles, and catenanes also behave in a very similar manner. Therefore, we report only the results obtained for the compounds derived from the polyether **6** – namely the pseudorotaxane **[6:13]**<sup>4+</sup>, the macrocyclic polyether **8**, and the catenane **11**<sup>4+</sup>.

#### Pseudorotaxane **[6:13]**<sup>4+</sup>

The electrochemical behavior of **[6:13]**<sup>4+</sup> on oxidation and reduction was studied in the presence of an excess of the cyclophane **13**<sup>4+</sup> and the polyether **6**, respectively, in order to obtain more than 95% of the electroactive species under investigation in the complexed form. The pseudorotaxane **[6:13]**<sup>4+</sup> shows two monoelectronic oxidation processes that can be attributed to the TTF-type unit of **6** (Figure 10). The anodic peak of the first process is displaced toward more positive potentials compared with the uncomplexed polyether because of the CT interaction that arises when the electron-donor TTF-type unit of **6** is threaded through the electron-accepting tetracationic cyclophane **13**<sup>4+</sup>; the second oxidation process, however, is not displaced. The first oxidation process is almost reversible for scan rates < 200 mV s<sup>-1</sup> and takes place (Figure 10a) at a potential 60 mV more positive compared with that for uncomplexed **6**; on increasing the scan rate, however, the anodic peak moves to more positive potentials, while the corresponding cathodic peak moves to less positive potentials. For a scan rate of 1000 mV s<sup>-1</sup> (Figure 10c), the latter peak is at a potential very close to that of the free acyclic polyether (Figure 10b). The second oxidation process of **[6:13]**<sup>4+</sup> is fully reversible (Figure 10). As previously observed<sup>[5b]</sup> for an adduct of **13**<sup>4+</sup> with a polyether containing a TTF unit, these results indicate that one-electron oxidation of the TTF-type unit of polyether **6** in **[6:13]**<sup>4+</sup> is followed by a dethreading process which occurs on the time scale of

the electrochemical experiment with the consequence that the second oxidation of the TTF-type unit occurs when dethreading has already taken place. Comparison with the behavior of the previously studied compound<sup>[5b]</sup> shows that, for the **[6:13]**<sup>4+</sup> pseudorotaxane, the dethreading movement is faster, since the positive shift of the first anodic peak is evident only for relatively high scan rates (> 200 mV s<sup>-1</sup>). On the other hand, the rethreading process seems to be slower, since for **[6:13]**<sup>4+</sup>, the reduction peak of the monooxidized wire occurs at a potential almost identical to that of free **6** for a scan rate of 1000 mV s<sup>-1</sup>. This observation means that, on this timescale, the monooxidized **6**<sup>+</sup> species, once reduced, has not enough time to enter back into the cavity of the tetracationic cyclophane. The lower limit for the anodic peak of **6**, when “locked” inside the **13**<sup>4+</sup> cyclophane, is given by the anodic peak (+0.70 V vs. SCE) obtained at the highest scan rate (1000 mV s<sup>-1</sup>).

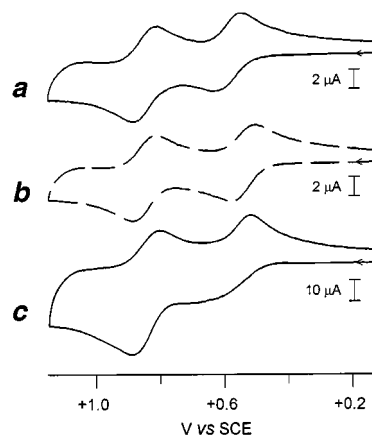


Figure 10. Cyclic voltammetric scan of a  $3.3 \cdot 10^{-4}$  M MeCN solution of **6** (i) alone (dashed line) and (ii) in the presence of an excess of **13**<sup>4+</sup> (full lines); the scan rate is 50 mV s<sup>-1</sup> for (a) and (b), and 1000 mV s<sup>-1</sup> for (c)

The two reversible, two-electron reduction processes characteristic<sup>[5b,7k]</sup> of cyclobis(paraquat-*p*-phenylene) cyclophane (**13**<sup>4+</sup>) are maintained in **[6:13]**<sup>4+</sup>. The first process occurs almost at the same potential as that observed for the free tetracationic cyclophane, while the second process is slightly shifted (ca. 20 mV) to more negative potentials. In the case of the above-mentioned adduct of **13**<sup>4+</sup> with a polyether containing a TTF unit,<sup>[5b]</sup> the first process was displaced to more negative potentials, as expected, because of the CT interaction. The apparently anomalous behavior observed for **[6:13]**<sup>4+</sup> can be accounted for by considering that the bulkiness of **6** could somewhat force coplanarity of the two pyridinium rings of each electron-acceptor unit of **13**<sup>4+</sup>, thereby favoring the formation of the planar monoreduced form.<sup>[20]</sup> The negative shift of the second reduction process of the **13**<sup>4+</sup> cyclophane in the **[6:13]**<sup>4+</sup> pseudorotaxane indicates that some residual charge-transfer interaction is still present after one-electron reduction of the cyclophane electron-acceptor units. This observation suggests that complete dethreading does not take place after one-

electron reduction of the cyclophane electron-acceptor units.

### Catenane $11^{4+}$

The cyclic polyether **8** shows two reversible and mono-electronic oxidation processes occurring at potentials (+0.53 V and +0.84 V vs. SCE) very similar to those of the corresponding acyclic parent compound **6**. The *p*-xylene unit is not electroactive in the potential window examined (−2/+2 V).

The [2]catenane  $11^{4+}$  shows two reversible and monoelectronic oxidation processes (+0.68 V and +0.90 V) that can be attributed to the TTF-type unit present in the macrocyclic polyether component (Figure 11). Both processes are shifted to more positive potentials with respect to the parent macrocyclic polyether, which is consistent with the CT interaction between the TTF-type unit and a nearby acceptor unit of the tetracationic cyclophane component. It should be noted, however, that a contribution to the potential shift can also come from an electrostatic repulsion between the positively charged unit of the cyclophane and the oxidized TTF-type unit of the polyether. The fact that the oxidation processes remain reversible in the catenanes is consistent with a structure where the TTF-type unit occupies an alongside position with respect to the tetracationic cyclophane. In the case of a structure in which the TTF-type unit is inside the tetracationic cyclophane component, the oxidation process would be expected to be affected by structural rearrangements,<sup>[5c]</sup> as observed for the corresponding  $[6:13]^{4+}$  pseudorotaxane.

As far as reduction is concerned, in catenane  $11^{4+}$  the two reversible two-electron processes characteristic of the free tetracationic cyclophane  $13^{4+}$  split (Figure 11) into four reversible one-electron processes (−0.26 V, −0.33 V, −0.82 V, −0.89 V, vs. SCE). The splitting of the first bielectronic wave is a result of the topological difference between inside and alongside electron-acceptor units of the tetracationic cyclophane in the catenane structure, as observed for all the other catenanes of this kind studied so far.<sup>[7k,21]</sup> The splitting observed for the second bielectronic wave indicates that the alongside/inside distinction for the two electron-acceptor units maintains some meaning, even after the first

reduction process.<sup>[7k]</sup> It should be noted that the first reduction process of the catenane occurs at a slightly less negative potential than the first reduction of the free  $13^{4+}$ . This result suggests that the catenane structure favors coplanarity of the two pyridinium rings of an electron-acceptor unit.<sup>[20]</sup> However, it is difficult to understand which unit (alongside or inside) is involved in the first reduction process. The following reduction processes are shifted toward more negative potentials compared with the free  $13^{4+}$ , showing the presence of some kind of electronic interactions and/or structural constraints.

### Conclusions

We have investigated two [2]pseudorotaxanes composed of acyclic polyethers containing a TTF-type unit threaded through the cavity of cyclobis(paraquat-*p*-phenylene) as well as two [2]catenanes composed of one of two macrocyclic polyethers, each containing a TTF-type unit, interlocked with this tetracationic cyclophane. The absorption spectra and the electrochemical properties of these complexes and compounds show that a CT interaction is present between the electron-donor TTF-type unit of the polyethers and the electron-acceptor units of the cyclophane. Oxidation of the TTF-containing guests from their neutral to their monocationic states dismembers the [2]pseudorotaxanes as a result of the disruption of the CT interaction and electrostatic repulsion between the tetracationic host and the monocationic guests. Reduction of the monocationic species to their neutral states is accompanied by the insertion of the regenerated neutral guests into the cavity of the host. These supramolecular systems can be regarded as prototypical molecular-sized machines which can be controlled by external redox stimuli. In the two [2]catenanes, the bis(2-oxy-1,3-propylenedithio)TTF unit resides preferentially alongside the cavity of the tetracationic cyclophane component whose interior is occupied by a *p*-xylene ring. The mechanically interlocked macrocyclic components of both [2]catenanes move relative to each other in solution while their mean planes undergo a mutual rocking motion – i.e., one ring precesses with respect to the other.

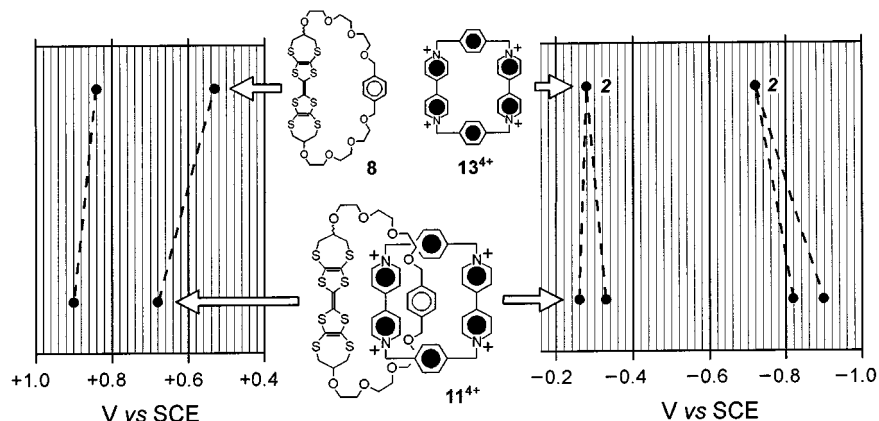


Figure 11. Correlation diagram for the halfwave potential values of **8**,  $13^{4+}$ , and the [2]catenane  $11^{4+}$

## Experimental Section

**General Methods:** Solvents were purchased from Aldrich and purified according to literature procedures.<sup>[22]</sup> Reagents were purchased from Aldrich except for **1**,<sup>[8]</sup> **10** · 2 PF<sub>6</sub>,<sup>[23]</sup> and **13** · 4 PF<sub>6</sub><sup>[24]</sup> which were synthesized according to literature procedures. – Thin layer chromatography (TLC) was carried out using aluminium sheets, precoated with silica gel 60F (Merck 5554) or aluminium oxide 60F<sub>254</sub> neutral (Merck 5550). The plates were inspected by UV light prior to development with iodine vapor or by treatment with ceric ammonium molybdate reagent and subsequent heating. – Melting points were determined with an Electrothermal 9200 apparatus and are uncorrected. – Electron impact mass spectra (EIMS) were recorded with a Kratos Profile spectrometer. Liquid secondary ion mass spectra (LSIMS) were recorded with a VG Zabspec triple-focussing mass spectrometer. – <sup>1</sup>H-NMR and <sup>13</sup>C-NMR spectra were recorded with a Bruker AC300 (300 and 75 MHz, respectively) spectrometer. All chemical shifts are quoted in ppm on the  $\delta$  scale using TMS or the solvent as an internal standard. – The absorption spectra were recorded with a Perkin–Elmer Lambda 40 spectrophotometer. Electrochemical experiments were carried out at room temperature in argon-purged MeCN solution, with a Princeton Applied Research 273 Multipurpose instrument interfaced to a PC. Both cyclic and differential pulse voltammetry techniques were used. Ru(bpy)<sub>3</sub><sup>2+</sup> [ $E_{1/2}(\text{Ru}^{3+}/\text{Ru}^{2+}) = +1.290$  V and  $E_{1/2}(\text{Ru}^{2+}/\text{Ru}^{+}) = -1.330$  V vs. SCE]<sup>[25]</sup> was present in the solution as an internal reference. The exact configuration and procedures for these experiments have been previously reported.<sup>[5b]</sup> The experimental error on the potential values is  $\pm 10$  mV. – Elemental analyses were performed by the University of North London Microanalytical Laboratories.

**1-Tosyl-10-(tetrahydropyran-2-yl)-1,4,7,10-tetraoxadecane (2) and 1-Tosyl-13-(tetrahydropyran-2-yl)-1,4,7,10,13-pentaoxatridecane (3):** A solution of 3,4-dihydro-2H-pyran (4.2 g, 50 mmol), either triethyleneglycol monotosylate (10.0, 32.9 mmol) or tetraethyleneglycol monotosylate (11.4 g, 32.8 mmol), and catalytic amounts of pyridinium *p*-toluenesulfonate in dry CH<sub>2</sub>Cl<sub>2</sub> (300 mL) was heated for 3 h under reflux and N<sub>2</sub>. After cooling down to ambient temperature, the mixture was poured into an aqueous solution of NH<sub>3</sub> (0.33%, 150 mL). The aqueous layer was extracted with CH<sub>2</sub>Cl<sub>2</sub> (4 × 100 mL). The combined organic layers were washed with H<sub>2</sub>O (4 × 100 mL), dried (MgSO<sub>4</sub>), and concentrated under reduced pressure to afford the product as a yellow oil. – **2** (16.2 g, 99%): LSIMS;  $m/z$ : 388 [M]<sup>+</sup>. – <sup>1</sup>H NMR (CDCl<sub>3</sub>):  $\delta$  = 7.72 (2 H, d,  $J$  = 8.5 Hz), 7.28 (2 H, d,  $J$  = 8.5 Hz), 4.60–4.54 (1 H, m), 4.15–4.08 (2 H, m), 3.82–3.74 (2 H, m), 3.65–3.38 (10 H, m), 2.37 (3 H, s), 1.85–1.40 (6 H, m). – <sup>13</sup>C NMR (CDCl<sub>3</sub>):  $\delta$  = 144.8, 133.0, 129.8, 127.9, 98.9, 70.7, 70.5, 70.5, 69.3, 68.6, 66.6, 62.2, 30.6, 25.4, 21.6, 19.5. – **3** (13.2 g, 90%): LSIMS;  $m/z$ : 455 [M + Na]<sup>+</sup>. – <sup>1</sup>H NMR (CDCl<sub>3</sub>):  $\delta$  = 7.75 (2 H, d,  $J$  = 8.5 Hz), 7.32 (2 H, d,  $J$  = 8.5 Hz), 4.60–4.54 (1 H, m), 4.15–4.08 (2 H, m), 3.85–3.75 (2 H, m), 3.65–3.40 (14 H, m), 2.40 (3 H, s), 1.82–1.42 (6 H, m). – <sup>13</sup>C NMR (CDCl<sub>3</sub>):  $\delta$  = 144.8, 133.0, 129.8, 128.0, 99.0, 72.5, 70.7, 70.5, 70.3, 69.3, 68.7, 66.7, 62.3, 61.7, 30.6, 25.4, 21.6, 19.5.

**Bis(2-{2-[2-(tetrahydropyran-2-yl)oxyethoxy]ethoxy}ethoxy-1,3-propylenedithio)tetrathiafulvalene (4) and Bis(2-{2-[2-(tetrahydropyran-2-yl)oxyethoxy]ethoxy}ethoxy-1,3-propylenedithio)tetrathiafulvalene (5):** A suspension of bis(2-hydroxy-1,3-propylenedithio)tetrathiafulvalene (**1**) (0.88 g, 2 mmol) and NaH (60% in mineral oil, 400 mg, 10 mmol) in dry and degassed THF (100 mL) was heated for 45 min under reflux and N<sub>2</sub>. A solution of either **2**

(3.90 g, 10 mmol) or **3** (4.48 g, 10 mmol) in dry and degassed THF (70 mL) was added over 2 h and the mixture was heated under reflux for further 24 h. After cooling down to ambient temperature, H<sub>2</sub>O was added and the solvent was removed under reduced pressure. The residue was partitioned between CH<sub>2</sub>Cl<sub>2</sub> (200 mL) and H<sub>2</sub>O (200 mL) and the aqueous layer was washed with CH<sub>2</sub>Cl<sub>2</sub> (2 × 50 mL). The combined organic layers were washed with H<sub>2</sub>O (3 × 100 mL) and dried (MgSO<sub>4</sub>). The solvent was removed under reduced pressure to afford a residue which was purified by column chromatography (SiO<sub>2</sub>, CH<sub>2</sub>Cl<sub>2</sub>/MeOH, 95:5) to yield the product either as a yellow solid (**4**) or as a yellow oil (**5**). – **4** (1.40 g, 80%): M.p. 88–90 °C. – LSIMS;  $m/z$ : 876 [M]<sup>+</sup>. – <sup>1</sup>H NMR (CDCl<sub>3</sub>):  $\delta$  = 4.66–4.60 (2 H, m), 3.90–3.80 (4 H, m), 3.73–3.47 (26 H, m), 3.03–2.90 (4 H, m), 2.60–2.35 (4 H, m), 1.88–1.48 (12 H, m). – <sup>13</sup>C NMR (CDCl<sub>3</sub>):  $\delta$  = 130.2, 112.4, 99.0, 83.4, 70.9, 70.8, 70.6, 69.1, 69.0, 66.7, 62.3, 36.7, 36.6, 30.6, 25.5, 19.6. – C<sub>34</sub>H<sub>52</sub>O<sub>10</sub>S<sub>8</sub> (877.308): calcd. C 46.58, H 5.94; found C 46.45, H 5.73. – **5** (1.54 g, 80%): LSIMS;  $m/z$ : 964 [M]<sup>+</sup>. – <sup>1</sup>H NMR (CDCl<sub>3</sub>):  $\delta$  = 4.66–4.60 (2 H, m), 3.90–3.80 (4 H, m), 3.70–3.45 (34 H, m), 2.98–2.88 (4 H, m), 2.58–2.32 (4 H, m), 1.90–1.45 (12 H, m). – <sup>13</sup>C NMR (CDCl<sub>3</sub>):  $\delta$  = 130.2, 99.0, 70.9, 70.8, 70.7, 70.6, 69.0, 66.7, 62.3, 36.7, 36.6, 30.6, 25.5, 19.5. – C<sub>38</sub>H<sub>60</sub>O<sub>12</sub>S<sub>8</sub> (965.420): calcd. C 47.30, H 6.22; found C 47.26, H 6.17.

**Bis{2-[2-(2-hydroxyethoxy)ethoxy]ethoxy-1,3-propylenedithio}-tetrathiafulvalene (6) and Bis(2-{2-[2-(2-hydroxyethoxy)ethoxy]ethoxy}ethoxy-1,3-propylenedithio)tetrathiafulvalene (7):** A suspension of either **4** (1.60 g, 1.8 mmol) or **5** (1.74 g, 1.8 mmol) and *p*-toluenesulfonic acid monohydrate (0.10 g, 0.5 mmol) in EtOH (95%, 150 mL) was heated for 24 h under reflux and N<sub>2</sub>. After cooling down to room temperature, the solvent was removed under reduced pressure and the residue was suspended in H<sub>2</sub>O (100 mL). After filtration, the solid was washed twice with MeCN (5 mL) to afford the product as a yellow solid. – **6** (1.23 g, 95%): M.p. 140–142 °C. – LSIMS;  $m/z$ : 708 [M]<sup>+</sup>. – <sup>1</sup>H NMR (CDCl<sub>3</sub>):  $\delta$  = 3.75–3.58 (26 H, m), 3.00–2.90 (4 H, m), 2.65–2.35 (6 H, m). – <sup>13</sup>C NMR (CDCl<sub>3</sub>):  $\delta$  = 130.3, 112.6, 83.5, 72.6, 70.9, 70.5, 69.0, 61.9, 36.7, 36.6. – C<sub>24</sub>H<sub>36</sub>O<sub>8</sub>S<sub>8</sub> (709.072): calcd. C 40.68, H 5.08; found C 40.64, H 4.88. – **7** (1.36 g, 95%): M.p. 96–100 °C. – LSIMS;  $m/z$ : 796 [M]<sup>+</sup>. – <sup>1</sup>H NMR (CDCl<sub>3</sub>):  $\delta$  = 3.90–3.55 (34 H, m), 3.03–2.93 (4 H, m), 2.65–2.35 (6 H, m). – <sup>13</sup>C NMR (CDCl<sub>3</sub>):  $\delta$  = 130.2, 112.0, 83.5, 72.5, 70.9, 70.7, 70.7, 70.6, 70.4, 69.0, 61.8, 36.7, 36.6. – C<sub>28</sub>H<sub>44</sub>O<sub>10</sub>S<sub>8</sub> (797.178): calcd. C 42.21, H 5.53; found C 42.29, H 5.61.

**Macrocyclic Polyethers 8 and 9:** A solution of either **6** (320 mg, 0.45 mmol) or **7** (358 mg, 0.45 mmol) and 1,4-bis(bromomethyl)benzene (119 mg, 0.45 mmol) in dry and degassed THF (125 mL) was added over 20 h to a suspension of NaH (60% in mineral oil, 200 mg, 5 mmol) in dry and degassed THF (100 mL) maintained at reflux under N<sub>2</sub>. The mixture was heated for further 20 h. After cooling down to room temperature, H<sub>2</sub>O was added and the THF was removed under reduced pressure. The resulting aqueous suspension was washed with CH<sub>2</sub>Cl<sub>2</sub> (5 × 100 mL) and the organic layer was washed with H<sub>2</sub>O (2 × 50 mL) and dried (MgSO<sub>4</sub>). The solvent was removed under reduced pressure and the residue was purified by column chromatography (SiO<sub>2</sub>, CH<sub>2</sub>Cl<sub>2</sub>/MeOH, 96:4) to afford the product as a yellow solid. – **8** (41 mg, 10%): M.p. 145–147 °C. – LSIMS;  $m/z$ : 810 [M]<sup>+</sup>. – <sup>1</sup>H NMR (CDCl<sub>3</sub>):  $\delta$  = 7.32 (4 H, s), 4.60 (4 H, m), 4.00–3.90 (2 H, m), 3.76–3.50 (24 H, m), 3.12–2.87 (4 H, m), 2.62–2.35 (4 H, m). – <sup>13</sup>C NMR (CDCl<sub>3</sub>):  $\delta$  = 137.6, 130.1, 128.0, 82.5, 73.3, 73.0, 71.6, 71.4, 70.9, 70.7, 69.5, 36.8. – C<sub>32</sub>H<sub>42</sub>O<sub>8</sub>S<sub>8</sub> (811.208): C 47.41, H 5.19; found C 47.05, H 4.89. – **9** (40 mg, 10%): M.p. 60–63 °C. – LSIMS;  $m/z$ : 898 [M]<sup>+</sup>. – <sup>1</sup>H NMR (CDCl<sub>3</sub>):  $\delta$  = 7.35–7.20 (4 H, m), 4.55 (2 H, br. s),



4.00–3.35 (36 H, m), 3.10–2.80 (4 H, m), 2.60–2.30 (4 H, m). –  $^{13}\text{C}$  NMR ( $\text{CDCl}_3$ ):  $\delta$  = 137.6, 130.1, 128.0, 73.1, 71.3, 70.7, 69.5, 36.7. –  $\text{C}_{36}\text{H}_{50}\text{O}_{10}\text{S}_8$  (899.314): calcd. C 48.11, H 5.57; found C 48.15, H 5.69.

**[2]Catenanes  $11 \cdot 4 \text{PF}_6$  and  $12 \cdot 4 \text{PF}_6$ :** A solution of  $10 \cdot 2 \text{PF}_6$  (110 mg, 0.16 mmol), 1,4-bis(bromomethyl)benzene (41 mg, 0.16 mmol), and either **8** (54 mg, 0.07 mmol) or **9** (63 mg, 0.07 mmol) in dry and degassed DMF (25 mL) was stirred for 21 d at ambient temperature and under  $\text{N}_2$ . The solvent was removed under reduced pressure and the residue was purified by preparative TLC ( $\text{SiO}_2$ ,  $\text{MeOH}/\text{MeNO}_2/\text{sat. NH}_4\text{PF}_6(\text{aq.})$ , 165:35:5) to afford the product as a green solid. –  $11 \cdot 4 \text{PF}_6$  (5 mg, 4%). – M.p. > 250 °C. – LSIMS;  $m/z$ : 1910  $[\text{M}]^+$ , 1765  $[\text{M} - \text{PF}_6]^+$ , 1620  $[\text{M} - 2 \text{PF}_6]^+$ , 1475  $[\text{M} - 3 \text{PF}_6]^+$ . –  $^1\text{H}$  NMR  $[(\text{CD}_3)_2\text{CO}]$ :  $\delta$  = 9.39 (8 H, d,  $J$  = 7.0 Hz), 8.33 (8 H, d,  $J$  = 7.0 Hz), 8.19 (8 H, s), 6.23 (8 H, br. s), 4.27–4.38 (4 H, m), 4.17 (4 H, br. s), 4.07–3.70 (28 H, m), 3.25–3.10 (4 H, m), 2.95–2.80 (4 H, m). –  $\text{C}_{68}\text{H}_{74}\text{F}_{24}\text{N}_4\text{O}_8\text{P}_4\text{S}_8$  (1911.760): calcd. C 42.72, H 3.90, N 2.93; found C 43.05, H 3.82, N 3.08. – Single crystals suitable for X-ray analysis were grown by vapor diffusion of  $\text{MeCO}_2\text{Et}$  into an MeCN solution of  $11 \cdot 4 \text{PF}_6$ . Crystal data:  $\text{C}_{68}\text{H}_{74}\text{F}_{24}\text{N}_4\text{O}_8\text{P}_4\text{S}_8 \cdot 3 \text{MeCO}_2\text{Et} \cdot \text{H}_2\text{O}$ ,  $M$  = 2194.0, triclinic,  $a$  = 11.653(8),  $b$  = 16.397(3),  $c$  = 27.884(7) Å,  $\alpha$  = 100.57(2),  $\beta$  = 95.90(3),  $\gamma$  = 105.56(4)°,  $V$  = 4980(4) Å<sup>3</sup>, space group  $P\bar{1}$ ,  $Z$  = 2,  $D_c$  = 1.463 g cm<sup>−3</sup>,  $\mu(\text{Cu-K}\alpha)$  = 3.202 mm<sup>−1</sup>,  $F(000)$  = 2264, 11081 independent reflections ( $2\theta < 120^\circ$ ) were collected with a Siemens P4 diffractometer, equipped with a rotating anode generator, at 203 K using  $\omega$ -scans and graphite-monochromated Cu-K $\alpha$  radiation. 6611 Reflections had  $|F_o| > 4 \sigma(F_o)$  and were considered to be observed. The structure was solved by direct methods. Severe disorder was observed in one of two polyether chains as a result of a formal configurational inversion at one of the bridgehead carbon atoms within the bis(2-oxy-1,3-propylenedithio)TTF unit. Disorder was also observed in one of the  $\text{PF}_6^-$  counterions. The disorder was resolved into two different orientations of reduced site-occupancy factors. While the macrocyclic polyether, the EtOAc solvent molecules, and the  $\text{PF}_6^-$  counterions were refined anisotropically, the tetracationic cyclophane and the  $\text{H}_2\text{O}$  molecule were refined isotropically. Full-matrix least-squares refinement on  $F^2$  gave  $R_1$  = 0.131 and  $wR_2$  = 0.321. Computations were carried out with an SGI-Indigo workstation using the SHELXTL package (version 5.03). Crystallographic data (excluding structure factors) for this structure have been deposited with the Cambridge Crystallographic Data Centre as supplementary publication number CCDC-103090. Copies of the data can be obtained free of charge on application to CCDC, 12 Union Road, Cambridge, CB2 1EZ, UK [Fax: (internat.) + 44-1223/336-033; E-mail: deposit@ccdc.cam.ac.uk]. –  $12 \cdot 4 \text{PF}_6$  (16 mg, 5%). – M.p. > 250 °C. – LSIMS;  $m/z$ : 1998  $[\text{M}]^+$ , 1853  $[\text{M} - \text{PF}_6]^+$ , 1708  $[\text{M} - 2 \text{PF}_6]^+$ , 1564  $[\text{M} - 3 \text{PF}_6]^+$ . –  $^1\text{H}$  NMR  $[(\text{CD}_3)_2\text{CO}]$ :  $\delta$  = 9.38 (8 H, d,  $J$  = 7.0 Hz), 8.32 (8 H, d,  $J$  = 7.0 Hz), 8.16 (8 H, br. s), 6.19 (8 H, br. s), 4.33–4.20 (2 H, m), 4.17 (4 H, br. s), 4.10–3.45 (36 H, m), 3.10–2.40 (8 H, m). –  $\text{C}_{72}\text{H}_{82}\text{F}_{24}\text{N}_4\text{O}_{10}\text{P}_4\text{S}_8$  (1999.866): calcd. C 43.24, H 4.13, N 2.80; found C 42.97, H 4.11, N 2.74.

## Acknowledgments

This research work was supported by the Engineering and Physical Sciences Research Council, the Deutsche Forschungsgemeinschaft, and the EU (contract FMRX-CT96-0076), MURST (Supramolecular Devices Project), and the Universities of Bologna (Funds for Selected Topics).

- [1] M. R. Bryce, *Chem. Soc. Rev.* **1991**, 20, 355–390.
- [2] For TTF-containing molecular and supramolecular systems, see: [2a] T. Jørgensen, T. K. Hansen, J. Becher, *Chem. Soc. Rev.* **1994**, 23, 41–51. – [2b] M. B. Nielsen, J. Becher, *Liebigs Ann.* **1997**, 2177–2187. – [2c] J. Becher, Z. T. Li, P. Blanchard, N. Svenstrup, J. Lau, M. B. Nielsen, P. Leriche, *Pure Appl. Chem.* **1997**, 69, 465–470. – [2d] M. R. Bryce, W. Devonport, L. M. Goldenberg, C. Wang, *Chem. Commun.* **1998**, 945–951.
- [3] For reviews on functioning molecular and supramolecular systems, see: [3a] V. Balzani, F. Scandola, *Supramolecular Photochemistry*, Horwood, Chichester, **1991**. – [3b] V. Balzani, *Tetrahedron* **1992**, 48, 10443–10514. – [3c] V. Balzani, M. Gómez-López, J. F. Stoddart, *Acc. Chem. Res.* **1998**, 31, 405–414. – [3d] R. A. Bissell, A. P. de Silva, H. Q. N. Gunaratne, P. L. M. Lynch, G. E. M. Maguire, K. R. A. S. Sandanayake, *Chem. Soc. Rev.* **1992**, 21, 187–195. – [3e] R. A. Bissell, A. P. de Silva, H. Q. N. Gunaratne, P. L. M. Lynch, G. E. M. Maguire, C. P. McCoy, K. R. A. S. Sandanayake, *Top. Curr. Chem.* **1993**, 168, 223–264. – [3f] A. P. De Silva, C. P. McCoy, *Chem. Ind.* **1994**, 992–996. – [3g] A. P. de Silva, H. Q. N. Gunaratne, T. Gunnlaugsson, A. J. M. Huxley, C. P. McCoy, J. T. Rademacher, T. E. Rice, *Chem. Rev.* **1997**, 97, 1515–1566. – [3h] P. D. Beer, *Adv. Inorg. Chem.* **1992**, 39, 79–157. – [3i] P. D. Beer, *Adv. Mater.* **1994**, 6, 607–609. – [3j] P. D. Beer, *Chem. Commun.* **1996**, 689–696. – [3k] P. D. Beer, *Acc. Chem. Res.* **1998**, 31, 71–80. – [3l] L. Fabbri, A. Poggi, *Chem. Soc. Rev.* **1995**, 24, 197–202. – [3m] M. D. Ward, *Chem. Ind.* **1997**, 640–645. – [3n] P. L. Boudas, M. Gómez-Kaifer, L. Echegoyen, *Angew. Chem. Int. Ed.* **1998**, 37, 216–247. – [3o] J.-P. Sauvage, *Acc. Chem. Res.* **1998**, 31, 611–619. – [3p] S. Shinkai, in *Comprehensive Supramolecular Chemistry* (Eds.: J. L. Atwood, J. E. D. Davies, D. D. Macnicol, F. Vögtle), Pergamon, Oxford, **1996**, vol. 1, pp. 671–700. – [3q] A. E. Kaifer, *Acc. Chem. Res.*, **1999**, 32, 62–71. – [3r] B. L. Feringa, W. F. Jager, B. de Lange, *Tetrahedron* **1993**, 49, 8267–8310.
- [4] [4a] D. Philp, A. M. Z. Slawin, N. Spencer, J. F. Stoddart, D. J. Williams, *J. Chem. Soc., Chem. Commun.* **1991**, 1584–1586. – [4b] P.-L. Anelli, M. Asakawa, P. R. Ashton, R. A. Bissell, G. Clavier, R. Görski, A. E. Kaifer, S. J. Langford, G. Mattersteig, S. Menzer, D. Philp, A. M. Z. Slawin, N. Spencer, J. F. Stoddart, M. S. Tolley, D. J. Williams, *Chem. Eur. J.* **1997**, 3, 1113–1135. – [4c] M. Devonport, M. A. Blower, M. R. Bryce, L. M. Goldenberg, *J. Org. Chem.* **1997**, 62, 885–887.
- [5] For examples of TTF-containing catenanes, rotaxanes, and pseudorotaxanes, see: [5a] P. R. Ashton, R. A. Bissell, N. Spencer, J. F. Stoddart, M. S. Tolley, *Synlett* **1992**, 923–926. – [5b] M. Asakawa, P. R. Ashton, V. Balzani, A. Credi, G. Mattersteig, O. A. Matthews, M. Montalti, N. Spencer, J. F. Stoddart, M. Venturi, *Chem. Eur. J.* **1997**, 3, 1992–1996. – [5c] M. Asakawa, P. R. Ashton, V. Balzani, A. Credi, C. Hamers, G. Mattersteig, M. Montalti, A. N. Shipway, N. Spencer, J. F. Stoddart, M. S. Tolley, M. Venturi, A. J. P. White, D. J. Williams, *Angew. Chem. Int. Ed.* **1998**, 37, 333–337. – [5d] T. Jørgensen, J. Becher, J.-C. Chambron, J.-P. Sauvage, *Tetrahedron Lett.* **1994**, 35, 4339–4342. – [5e] Z. T. Li, P. C. Stein, N. Svenstrup, K. H. Lund, J. Becher, *Angew. Chem., Int. Ed. Engl.* **1995**, 34, 2524–2528. – [5f] Z. T. Li, J. Becher, *Chem. Commun.* **1996**, 639–640. – [5g] Z. T. Li, P. C. Stein, J. Becher, D. Jensen, P. Mørk, N. Svenstrup, *Chem. Eur. J.* **1996**, 2, 624–633. – [5h] Z. T. Li, J. Becher, *Synlett* **1997**, 557–560. – [5i] M. B. Nielsen, N. Thorup, J. Becher, *J. Chem. Soc., Perkin Trans. 1* **1998**, 1305–1308. – [5j] A. Credi, M. Montalti, V. Balzani, S. J. Langford, F. M. Raymo, J. F. Stoddart, *New J. Chem.* **1998**, 22, 1061–1065.
- [6] For reviews on mechanically interlocked molecules, see: [6a] C. O. Dietrich-Buchecker, J.-P. Sauvage, *Bioorg. Chem. Front.* **1991**, 2, 195–248. – [6b] J.-C. Chambron, C. O. Dietrich-Buchecker, J.-P. Sauvage, *Top. Curr. Chem.* **1993**, 165, 131–162. – [6c] H. W. Gibson, H. Marand, *Adv. Mater.* **1993**, 5, 11–21. – [6d] H. W. Gibson, M. C. Bheda, P. T. Engen, *Prog. Polym. Sci.* **1994**, 19, 843–945. – [6e] F. Vögtle, T. Dünwald, T. Schmidt, *Acc. Chem. Res.* **1996**, 29, 451–460. – [6f] R. Jäger, F. Vögtle, *Angew. Chem., Int. Ed. Engl.* **1997**, 36, 930–944. – [6g] D. B. Amabilino, J. F. Stoddart, *Chem. Rev.* **1995**, 95, 2725–2828. – [6h] M. Belohradsky, F. M. Raymo, J. F. Stoddart, *Collect. Czech. Chem. Commun.* **1996**, 61, 1–43. – [6i] M. Belohradsky, F. M. Raymo, J. F. Stoddart, *Collect. Czech. Chem. Commun.* **1997**, 62, 527–557. – [6j] S. A. Nepogodiev, J. F. Stoddart, *Chem. Rev.* **1998**, 98, 1959–1976.

- [7] For examples of redox-controlled molecular movements in catenanes, rotaxanes, and pseudorotaxanes, see refs. [5b,5c,5] and: [7a] A. Livoreil, C. O. Dietrich-Buchecker, J.-P. Sauvage, *J. Am. Chem. Soc.* **1994**, *116*, 9399–9400. — [7b] D. B. Amabilino, C. O. Dietrich-Buchecker, A. Livoreil, L. Pérez-García, J.-P. Sauvage, J. F. Stoddart, *J. Am. Chem. Soc.* **1996**, *118*, 3905–3913. — [7c] D. J. Cárdenas, A. Livoreil, J.-P. Sauvage, *J. Am. Chem. Soc.* **1996**, *118*, 11980–11981. — [7d] F. Baumann, A. Livoreil, W. Kaim, J.-P. Sauvage, *Chem. Commun.* **1997**, 35–36. — [7e] A. Livoreil, J.-P. Sauvage, N. Armaroli, V. Balzani, L. Flamigni, B. Ventura, *J. Am. Chem. Soc.* **1997**, *119*, 12114–12124. — [7f] A. Diaz, P. A. Quintela, J. M. Schuette, A. E. Kaifer, *J. Phys. Chem.* **1988**, *92*, 3537–3542. — [7g] R. A. Bissell, E. Córdova, A. E. Kaifer, J. F. Stoddart, *Nature* **1994**, *369*, 133–137. — [7h] E. Córdova, R. A. Bissell, A. E. Kaifer, *J. Org. Chem.* **1995**, *60*, 1033–1038. — [7i] A. Mirzozian, A. E. Kaifer, *Chem. Eur. J.* **1997**, *3*, 1052–1058. — [7j] R. Castro, L. A. Godínez, C. M. Criss, A. E. Kaifer, *J. Org. Chem.* **1997**, *62*, 4928–4935. — [7k] P. R. Ashton, R. Ballardini, V. Balzani, A. Credi, M. T. Gandolfi, S. Menzer, L. Pérez-García, L. Prodi, J. F. Stoddart, M. Venturi, A. J. P. White, D. J. Williams, *J. Am. Chem. Soc.* **1995**, *117*, 11171–11197.
- [8] Compound **1** was obtained as a mixture of the *cis* and the *trans* isomers. This mixture was employed as the starting material in subsequent reactions and compounds **4–12** · 4 PF<sub>6</sub> were also all obtained as mixtures of their *cis* and *trans* isomers. All the attempts to separate the two isomers of these compounds were unsuccessful. For the synthesis of **1**, see: G. J. Marshall, M. R. Bryce, G. Cooke, T. Jørgensen, J. Becher, C. D. Reynolds, S. Wood, *Tetrahedron* **1993**, *49*, 6849–6862.
- [9] The mean interplanar separations between the encircled *p*-xylene ring and the “inside” and “alongside” bipyridinium units are 3.67 and 3.60 Å, respectively. The centroid–centroid separations between the *p*-xylene ring of the macrocyclic polyether and the *p*-xylene rings of the tetracationic cyclophane are 5.16 and 4.96 Å. The associated H···π distances are 2.83 and 2.67 Å and the corresponding C–H···π angle is 162° in both cases.
- [10] The C···O, H···O distances [Å] and C–H···O angles [°] are 3.36, 2.44, 161 and 3.38, 2.47, 157, respectively.
- [11] For examples of S···N interactions, see: [11a] I. Jalsovszky, O. Farkas, O. Rabai, A. Kucsman, *Theochem – J. Mol. Struct.* **1996**, *365*, 93–102. — [11b] I. Jalsovszky, O. Farkas, A. Kucsman, *Theochem – J. Mol. Struct.* **1997**, *418*, 155–163.
- [12] The intracatenane separation between the C=C bond of the TTF unit and the C–C bond linking the two pyridinium rings of the “inside” bipyridinium unit is 3.76 Å.
- [13] [13a] P. R. Ashton, S. Menzer, F. M. Raymo, G. K. H. Shimizu, J. F. Stoddart, D. J. Williams, *Chem. Commun.* **1996**, 487–490. — [13b] M. Asakawa, P. R. Ashton, S. Menzer, F. M. Raymo, J. F. Stoddart, A. J. P. White, D. J. Williams, *Chem. Eur. J.* **1996**, *2*, 877–893.
- [14] In the <sup>1</sup>H-NMR spectra of **4–12** · 4 PF<sub>6</sub>, the bis(2-oxy-1,3-propylenedithio)TTF protons give rise to complex patterns since the isomerization between the *cis* and the *trans* isomers is slow on the <sup>1</sup>H-NMR timescale.
- [15] The EXSY spectra of **11** · 4 PF<sub>6</sub> and **12** · 4 PF<sub>6</sub> recorded at 193 K show exchange occurring between all the environmental subsets associated with the bipyridinium units and with the encircled *p*-xylene ring. Thus, the existence of these environmental subsets cannot be a consequence of the *cis/trans* isomerism (ref. [14]): Rather, it is a result of both Processes I and II being slow on the <sup>1</sup>H-NMR timescale at this temperature.
- [16] Rough estimates of the energy barriers associated with Processes I and II were derived by employing the approximate coalescence method. For both [2]catenanes, values of ca. 10 kcal mol<sup>−1</sup> were obtained from all the coalescing pairs of resonances. For a discussion of the approximate coalescence method, see: I. O. Sutherland *Annu. Rep. NMR Spectrosc.* **1971**, *4*, 71–235.
- [17] The liquid secondary ion mass spectrum (LSIMS) of an equimolar CD<sub>3</sub>CN/D<sub>2</sub>O (95:5) solution of **6** and **13** · 4 PF<sub>6</sub> shows peaks at *m/z* values of 1664 and 1519 for [M – PF<sub>6</sub>]<sup>+</sup> and [M – 2 PF<sub>6</sub>]<sup>+</sup>, respectively. These peaks correspond to the consecutive losses of one and two PF<sub>6</sub><sup>−</sup> counterions from the 1:1 complex [6:13] · 4 PF<sub>6</sub>. By contrast, the LSIMS recorded after the addition of I<sub>2</sub> – i.e., after the oxidation of the TTF unit to the radical monocation – does not show the peaks corresponding to the complex. However, an LSIMS, identical to that of the original solution, is obtained after the addition of Na<sub>2</sub>S<sub>2</sub>O<sub>5</sub>/NH<sub>4</sub>PF<sub>6</sub>/D<sub>2</sub>O – i.e., after reducing the TTF unit back to its neutral state.
- [18] [18a] S. Hünig, G. Kießlich, H. Quast, D. Scheutzw, *Liebigs Ann. Chem.* **1973**, 310–323. — [18b] G. Schukat, E. Fanghänel, *J. Prakt. Chem.* **1985**, *327*, 767–774.
- [19] P. R. Ashton, V. Balzani, J. Becher, A. Credi, M. C. T. Fyfe, G. Mattersteig, S. Menzer, M. B. Nielsen, F. M. Raymo, J. F. Stoddart, M. Venturi, D. J. Williams, *J. Am. Chem. Soc.*, in press.
- [20] P. Wardman, *J. Phys. Chem. Ref. Data* **1989**, *18*, 1637–1755.
- [21] R. Ballardini, V. Balzani, A. Credi, C. L. Brown, R. E. Gillard, M. Montalti, D. Philp, J. F. Stoddart, M. Venturi, A. J. P. White, B. J. Williams, D. J. Williams, *J. Am. Chem. Soc.* **1997**, *119*, 12503–12513.
- [22] D. D. Perrin, W. L. Armarego, *Purification of Laboratory Chemicals*, 3rd ed., Pergamon Press, New York, **1988**.
- [23] P.-L. Anelli, P. R. Ashton, R. Ballardini, V. Balzani, M. Delgado, M. T. Gandolfi, T. T. Goodnow, A. E. Kaifer, D. Philp, M. Pietraszkiewicz, L. Prodi, M. V. Reddington, A. M. Z. Slawin, N. Spencer, J. F. Stoddart, C. Vicent, D. J. Williams, *J. Am. Chem. Soc.* **1992**, *114*, 193–218.
- [24] M. Asakawa, W. Dehaen, G. L’abbé, S. Menzer, J. Nouwen, F. M. Raymo, J. F. Stoddart, D. J. Williams, *J. Org. Chem.* **1996**, *61*, 9591–9595.
- [25] A. Juris, V. Balzani, F. Barigelli, S. Campagna, P. Belser, A. von Zelewsky, *Coord. Chem. Rev.* **1988**, *84*, 85–277.

Received December 14, 1998  
[O98555]